

Room Temperature Hydrogen Detection Using 1-D Nanostructured Tin Oxide Sensor

S. Deshpande^{1,2}, A. Karakoti^{1,2}, G. Londe^{1,2}, H. J. Cho^{1,2}, and S. Seal^{1,2,*}

¹Advanced Materials Processing and Analysis Center (AMPAC) and ²Mechanical Materials and Aerospace Department (MMAE), 4000, Central Florida Boulevard, Orlando, FL 32816, USA

Room temperature sensing of hydrogen using randomly oriented tin oxide nanowires has been demonstrated successfully. The role of surface functionalization of nanowires with platinum catalyst in rapid hydrogen detection is also studied. These nanowires were successfully incorporated into a micro-electro-mechanical (MEMS) device. The device can successfully detect hydrogen gas (as low as 500 ppm) with response time as low as 10 sec. Effect of aspect ratio of the nanowires on diffusion of hydrogen molecules in the tin oxide nanowires is elucidated in detail.

Keywords: Tin Oxide Nanowires, MEMS, Hydrogen Sensor, Room Temperature Detection.

Due to their captivating properties such as high surface to volume ratio, better crystallinity, ability to modulate their properties by varying dimensions, one dimensional nanostructures (ODNS) are subject area of intensive research.^{1,2} Especially in the field of gas sensing, where interaction of gases (analyte) with detecting material is a surface phenomenon, ODNS offer the advantage of providing high surface area compared to their other nanostructure counterparts. Till date various one dimensional metal/metal oxide nanostructures have been explored for the gas sensing applications. Tin oxide (SnO_2) is a well known *n*-type semiconductor gas sensor. Gas sensing characteristics of nanostructured tin oxide appears to be well established. However, literature indicates that most of the research conducted till now has been concentrated in the high temperature region (greater than 100 °C).³ Most of the industrial applications demand the gas sensor to be operated at lower temperature to avoid instability in nanocrystalline size, and hence, to increase the robustness and the life of the sensor.

At room temperature detection of hydrogen high response and recovery time is the major issue, which is yet to be resolved. It has been recently reported that, out of various morphologies of SnO_2 , such as single nanowire, porous mesh of randomly oriented nanowires, and thin films, highest gas sensitivity is achieved using the thin film form of the sensor.⁴ However, minimum response time is demonstrated by the single nanowire form of the sensor well known as field effect transistor (FET).^{5,6} But, the porous mesh of randomly oriented SnO_2 nanowires (TNW)

is likely to give moderate gas sensitivity with reasonably lower detection time. Hence, much attention has been given to synthesis of randomly oriented porous structure of SnO_2 using different processing techniques.^{7–9} In present work TNW have been synthesized via thermal evaporation technique and integrated successfully with MEMS device. This sensor device have shown fast response and recovery as well as enhanced sensitivity at room temperature.

In the present study TNW has been synthesized via thermal evaporation technique, explained in detail elsewhere.¹⁰ In short, Nanowires of SnO_2 were grown in a tube furnace by thermal evaporation of Stannous Oxide (SnO) on Si/SiO_2 substrate at 900 °C in Argon(Ar) atmosphere. Formation of ODNS depends on the formation of liquid alloy with platinum catalyst, vapor–solid–liquid interfacial energy, distribution of inert gases and inertness of reactant products.¹¹

The structural and morphological evolution of as synthesized TNW was studied using high-resolution transmission electron microscopy (HR-TEM) using Philips Technai G² TEM and the scanning electron microscope (JSM-6400F, JEOL, Tokyo, Japan). Typical SEM images of the as synthesized TNW deposited on the Si/SiO_2 substrates as a function of platinum (Pt) sputtering time at the processing temperature of 900 °C are presented in Figure 1 (inset). Randomly oriented, straight and long nanowires, as long as 50 μm , are formed under these processing conditions. From Figure 1 it can be concluded that the Pt sputtering time can affect the diameter of the nanorods. Longer Pt sputtering time results in formation of large size Pt nanoparticle which subsequently acts as catalyst particles for the growth of SnO_2 rods. But larger Pt

* Author to whom correspondence should be addressed.

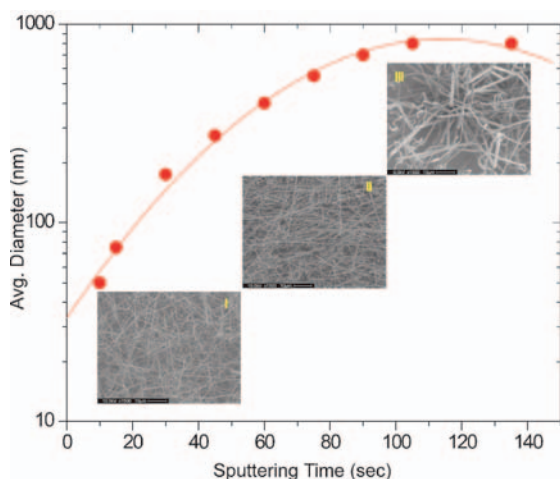


Fig. 1. Effect of platinum sputtering time on the nanowire diameter. Inset showing SEM images of the nanowire on SiO₂ substrate for platinum sputtering time (i) 15 s (ii) 45 s (iii) 90 s

nanoparticle reduces the surface coverage of the nanorods and a 120 s Pt sputtering time resulted in thin film of faceted nanoparticles. Figures 2(a–b) shows TEM image of a SnO₂ nanowire with a diameter around 25 nm. High resolution image of SnO₂ Figure 2 indicates the formation of SnO₂ nanorods without any catalyst particle at the tip. In the present scenario, nanorod growth occurs via vapor–solid (VS) mechanism (also known as ‘oxide-assisted-growth’ mechanism). In this mechanism, the initial Pt-catalyst particle assists in the formation of a thin film of faceted SnO₂ nanoparticles. These SnO₂ nanoparticles then act as nuclei for the growth of the TNW via direct deposition of Sn and O atoms from the vapor phase on their surfaces.

Integration of nanostructures with the micro-electro-mechanical devices (MEMS) is a rigorous task. In present study the contact pads were fabricated on the top of TNW grown on Si/SiO₂ substrate by thermal evaporation (Fig. 3(a)). A shadow mask was used to form the contact pattern. The shadow mask was made out of thick polyamide tape. The shape of the contact pad was cut out on the polyamide tape. Metallization was performed at a high vacuum of 3×10^{-5} Torr. The chamber was evacuated by a cryo pump. Initially a chromium (Cr) seed layer of around 100 Å was deposited followed by the gold (Au) layer of around 1000 Å. The Cr seed layer is used to ensure that the Au adheres to the surface. The sensor, with the fabricated Au contact pads, was mounted on a ceramic package. The sensor contacts were connected to the package contacts and the conductivity was tested. Prior to pad development procedure Pt was sputtered on as synthesized tin oxide nanowires for 15 seconds (~15 A). Sensor testing of the sensor was measured at room temperature under low pressure ($P = 50$ Torr) and dynamic air environment.

A typical response transient of tin oxide nanowires is shown in Figure 3(b). SnO₂ being a *n* type semiconductor, its electronic conductivity at room temperature is governed

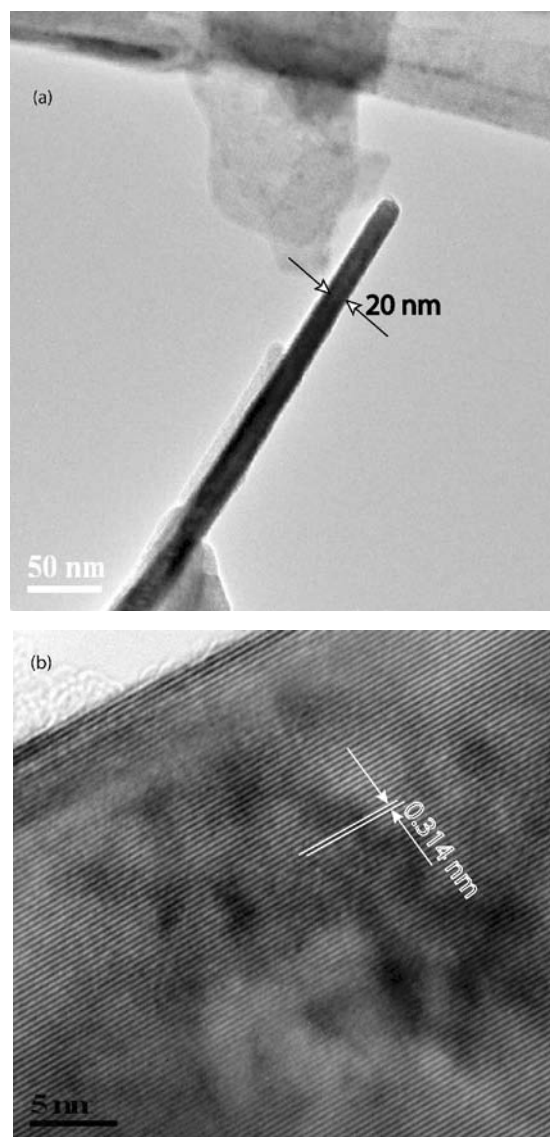
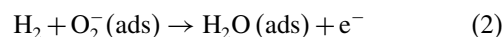
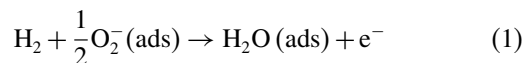


Fig. 2. (a–b) High resolution transmission electron microscopy (HR-TEM) images of the thermally grown SnO₂ nanowires.

by the generation of oxygen-ion vacancies. When a SnO₂ is exposed to air, physisorbed O₂ molecules pick-up the electrons from conduction band and change to O_{2ads}⁻ and O_{ads}⁻ species. Consequently a space charge layer (an electric double layer) is formed near the surface of SnO₂. Upon exposure of the film to a reducing gas such as hydrogen, the gas get oxidized via reaction with the O_{2ads}⁻ or O_{ads}⁻ species, subsequently, electrons are reintroduced into the space charge layer.^{12,13}



As a result, sensor resistance diminishes in the presence of hydrogen. Pristine tin oxide nanowires show very little sensitivity (even negligible) towards hydrogen. Inset in

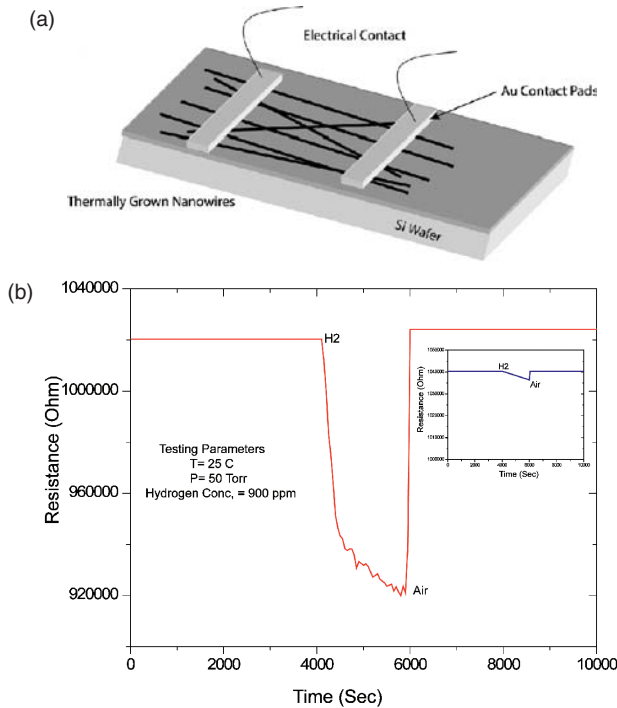


Fig. 3. (a) Figure showing the schematic of contact geometry for multiple-nanorod gas sensor. (b) Response transient of the thermally grown nanowire sensor device to 900 ppm hydrogen at room conditions.

Figure 3(b) shows the effect of presence of platinum on the sensor device. Presence of Pt on nanowire surfaces act as a catalyst for hydrogen dissociation. Previous studies have shown that hydrogen adsorption energy is lowest on Pt surface than Ni and Pd.^{14, 15}

Figure 4 represents the effect of hydrogen concentration (500–3000 ppm) on the response time and sensitivity at room temperature of TNW sensor of different diameters. Response time of almost 10 s was shown by sensor device having TNW with 30 nm diameter. While, sensitivity increased almost 10 times ($R_a/R_g = 0.4$ to 4) with increase in hydrogen concentration from 500 ppm to

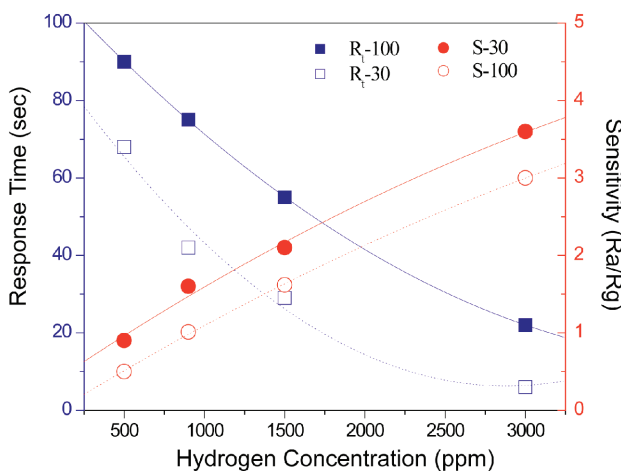


Fig. 4. Sensitivity and response time of the thermally grown nanowires having different nanowire diameter.

3000 ppm. The sensors were capable of detecting hydrogen in the range of ppm at room temperature and shows quick response and recovery. Lower sensitivity observed in present testing can be ascribed to lower operating temperature of the gas sensor. At lower operating temperatures ($<100\text{ }^\circ\text{C}$), the $\text{O}_{2\text{ads}}^-$ ions are adsorbed in preference to O_{ads}^- ions on the SnO_2 surface. $\text{O}_{2\text{ads}}^-$ ion being less reactive species with H_2 than O_{ads}^- ions result in lowering the sensor sensitivity towards hydrogen. Also, the activation energy for molecular H_2 dissociation into atomic H increases with decreasing operating temperature. This increased activation energy impede the H_2 sensitivity at lower operating temperatures.

Figure 4 shows the effect of diameter of nanowires on the overall hydrogen sensing performance. The response kinetics of the sensor device is dependant on the hydrogen diffusion into the nanowire. Electro-neutrality is maintained by the charge transfer between the hydrogen molecule and specific active site and this leads to increase in charge carrier density. We can describe this process with a model of diffusion in the solid cylinder with constant gas surface concentration. For a nanowire having radius “ r ” concentration variation inside the nanowire can be given by:¹⁶

$$C(t)/C_0 = 1 - \sum_{n=1}^{\infty} \frac{4}{\alpha_n^2} e^{-D \cdot \alpha_n^2 \cdot t/d^2} \quad (3)$$

Where, C_0 is the initial surface concentration. D is the apparent diffusion coefficient, t is time, and d is the average diameter of nanowire. α_n are the roots of $J(\alpha_n) = 0$, where J is the Bessel function of the first kind of order zero. Considering the constant diffusion coefficient, Figure 5 shows the faster concentration variation inside the nanowire having 30 nm diameter to sensor having diameter of 100 nm. This leads to better performance of sensor device having 30 nm diameter as compared to the sensor device with 100 nm diameter.

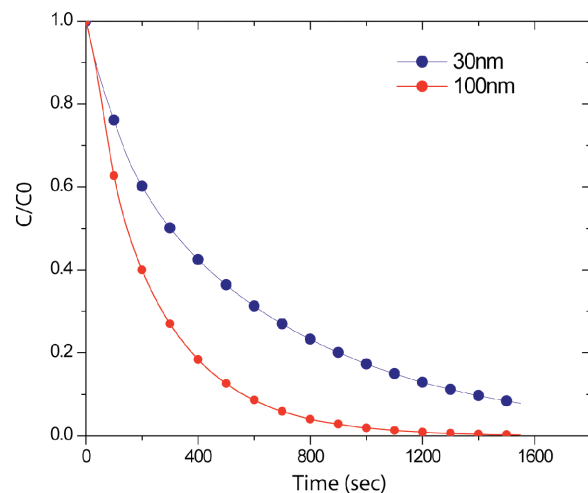


Fig. 5. Effect of concentration variation on nanotube with respect to time. Faster diffusion of hydrogen inside the small diameter nanowires leads the faster response kinetics and enhanced sensor performance.

In conclusion, tin oxide nanowires were successfully synthesized using oxide assisted growth mechanism. The size of the nanorods was found to be dependent on the function of substrate coverage of catalyst which governs the final diameter of the nanorods. These nanorods were successfully incorporated in the MEMS device. TNWS sensor successfully detected hydrogen with response time as low as 10 s at room temperature.

The authors would like to thank NASA-Glenn, ASRC Corporation and NSF-CTS for funding nanotechnology and sensor research.

References and Notes

1. S. V. N. T. Kuchibhatla, A. Karakoti, D. Bera, and S. Seal, *Prog. Mater. Sci.* (2007), in press.
2. Y. Cui and C. Lieber, *Science* 291, 851 (2001).
3. S. Shukla and S. Seal, Encyclopedia of Sensors, edited by C. Grimes, E. Dickey, and M. Pishko, American Scientific Publishers, Los Angeles (2006), Vol. 5, p. 379.
4. S. Shukla, P. Zhang, H. J. Cho, S. Seal, and L. Ludwig, *Sens. Actuators B* 120, 573 (2007).
5. A. Kolmakov, D. O. Klenov, Y. Lilach, S. Stemmer, and M. Moskovits, *Nano Lett.* 5, 667 (2005).
6. D. Zhang, Z. Liu, C. Li, T. Tang, X. Liu, S. Han, B. Lei, and C. Zhou, *Nano Lett.* 4, 1919 (2004).
7. Y. Wang and J. Y. Lee, *J. Phys. Chem. B* 108, 17832 (2004).
8. W. Zhu, W. Wang, H. Xu, and J. Shi, *Mater. Chem. Phys.* 99, 127 (2006).
9. Y. J. Chen, X. Y. Xue, Y. G. Wang, and T. H. Wang, *Appl. Phys. Lett.* 87, 233503 (2003).
10. S. Shukla, V. Venkatachalapathy, and S. Seal, *J. Phys. Chem. B* 110, 11210 (2006).
11. V. A. Nebol'sin and A. A. Shchetinin, *Inorg. Mater.* 39, 899 (2003).
12. S. Shukla and S. Seal, *J. Nanosci. Nanotechnol.* 4, 141 (2004).
13. M.-I. Baraton, L. Merhari, H. Ferkel, and J.-F. Castagnet, *Mater. Sci. Eng. C* 19, 315 (2002).
14. H. T. Wang, B. S. Kang, F. Ren, L. C. Tien, P. W. Sadik, D. P. Norton, S. J. Pearton, and J. Lin, *Appl. Phys. A* 81, 1117 (2005).
15. W. Eberhardt, F. Greunter, and E. W. Plummer, *Phys. Rev. Lett.* 46, 1085 (1981).
16. J. Crank, *The Mathematics of Diffusion*, The Clarendon press, Oxford (1955).